Catal Lett (2008) 124:74–79
DOI 10.1007/s10562-008-9485-6

CO Oxidation Activity of Ag/TiO$_2$ Catalysts Prepared via Oxalate Co-precipitation

Krisztina Frey · Viacheslav Iablokov ·
Gérôme Melaet · László Guczi · Norbert Kruse

Received: 19 February 2008 / Accepted: 1 April 2008 / Published online: 19 April 2008

Abstract Ag/TiO$_2$ catalysts with different Ag loadings (2, 4, 7 and 10% (w/w)) have been prepared by means of co-precipitation of Ag- and TiO-oxalates followed by temperature programmed oxidation (TPO). The catalysts were subjected to CO oxidation in a flow reactor at atmospheric pressure and temperatures up to 573 K. Best conversion performance was obtained in a CO/O$_2$ = 1:1 mixture over 10% Ag/TiO$_2$ for which the temperature of 50% CO conversion was $T_{50} = 333$ K. The initial reaction rates were determined in a circulation reactor at low conversions and apparent activation energies between 13 and 25 kJ/mol were found for all catalysts. Transmission electron microscopy shows a broad range of nano-sized Ag particles on TiO$_2$ (nearly pure anatase).

Keywords Ag · TiO$_2$ · Oxalates · Co-precipitation · Catalytic activity · CO oxidation

1 Introduction

Gold-based catalysts are currently setting the standard for high activity performance in CO oxidation. As was shown first by Haruta et al. [1] nanometer-sized Au particles supported on various metal oxides of the first transition period, demonstrated activity for this reaction at temperatures as low as 195 K. Au/TiO$_2$ catalysts were reported to be particularly active [2] but no general consensus seems to have been reached as to why this particular metal-support combination performs best. On the other hand, the size [3] and the morphological shape [4] of the Au nano-particles obviously play a vital role and so do surface defects of the titania support which strongly interact with the Au nanoparticles thereby causing significant charge transfer between the support and the noble metal [4–6]. For a summary of the present state of knowledge see ref. [7].

Comparatively much less information is currently available on the performance of Ag-supported catalysts in the same reaction. Sarkany [8] observed 50% CO conversion over Ag/Al$_2$O$_3$ at 523 K while Lippits et al. [9], in a comparative study with group Ib noble metals on γ-Al$_2$O$_3$, reported rather strongly varying data depending on the method of preparation. The authors stated gold catalysts to be most active among these metals, followed by Cu and Ag. Interestingly, for a Ag-based catalyst prepared by homogeneous deposition-precipitation the initially high activity was followed by rapid deactivation at temperatures above 523 K. Ag particles in this catalyst were reported to have diameters of less than 3 nm. On the other hand, catalysts prepared by liquid phase reduction turned out to be less active at low temperature but stable above 523 K where 100% CO conversion was observed. The Ag particle sizes in this latter case were in the range of 8–9 nm. Initially high reaction rates in CO oxidation were also reported by Qu et al. [10] in work on silica-supported Ag catalysts. The same authors claimed Ag particle sizes of 6–8 nm to yield the highest activity. Moreover, the pre-treatment procedure of these catalysts seemed to have a strong influence on the low-temperature activity. Unfortunately, no information was provided on the high-temperature stability of these

---

K. Frey · V. Iablokov · G. Melaet · N. Kruse
Chemical Physics of Materials, Université Libre de Bruxelles,
Campus Plaine, CP 243, 1050 Brussels, Belgium

K. Frey (✉) · L. Guczi
Department of Surface Chemistry and Catalysis,
Institute of Isotopes, Konkoly Thege Miklós út 29/33,
1121 Budapest, Hungary
e-mail: frey@sunserv.kfki.hu

catalysts. Kinetic studies of the CO oxidation in the presence of hydrogen failed to reach 100% CO conversion. Instead, after passing through a low-temperature maximum, the conversion generally decreased at temperatures starting already below 373 K depending on the actual catalyst composition [11].

It seems that little attention has as yet been devoted to the CO oxidation over Ag particles on reducible oxide supports such as TiO_2, Mn_2O_3 and others. In work by Imamura et al. [12], manganese–silver (70/30) composite oxides were found to yield 50% CO conversion at temperatures around 373 K. Subsequent work by Xia et al. [13] with considerably lower Ag amounts on a MnO_x-derived support has also shown low-temperature CO oxidation activity.

The present work is aimed at producing active Ag/TiO_2 catalysts by co-precipitation of Ag- and TiO-oxalates followed by temperature programmed oxidation (TPO). Since this preparation route is rather new it will be described in detail. It will be demonstrated that such Ag/TiO_2 catalysts provide high conversion in the CO oxidation at temperatures ranging between slightly above room temperature and at least 523 K.

2 Experimental

Ag/TiO_2 catalysts were prepared by oxalate co-precipitation using $AgNO_3$ and $Ti(OCH(CH_3)_2)_4$ as precursors. We note that the method is also well suited to prepare active catalysts by co-precipitation of transition metals other than Ag [14]. In the present work various amounts of $AgNO_3$ were dissolved in acetone while gently heating up to 313 K in an ultrasonic bath. $Ti(OCH(CH_3)_2)_4$ was added after its dissolution in acetone (before removal from the ultrasonic bath) followed by co-precipitation at 313 K using oxalic acid (10-fold excess as compared to stoichiometric amounts) while stirring vigorously. The co-precipitation was instantaneous. After 4–5 min the precipitate/acetone slurry was kept for sedimentation during 2 h while darkening. Subsequent centrifugation, washing in acetone and drying at 318 K overnight in an oven produced the mixed oxalate precursor with a white colour. Ag loadings in the catalysts were 2, 4, 7 and 10% (w/w). A TiO_2 sample was prepared in the same way and used as a reference sample.

Oxalate precursors were transformed into active catalysts using temperature programmed oxidation (TPO). A heating rate of 3 K/min was applied while passing 10% O_2 in argon at a volumetric rate of 50 mL/min across the sample bed (deposited on a frit inside the reactor). Once the maximum temperature of 798 K was reached, the sample was kept in the O_2/Ar gas flow during 20 min. After terminating the activation, the catalyst was cooled to room temperature in flowing O_2/Ar. During activation the sample weight was reduced by about 60%. The TPO activation was performed in situ in the same (pyrex) reactor that was also used for CO oxidation studies. After the TPO activation the gas flow was switched to a $CO + O_2$ mixture of 2% each, using Ar as diluent with a flow rate of 50 mL/min. The temperature was increased incrementally (10 K/min) while time intervals of 20 min were kept between successive temperature increments. The down-stream gas composition was continuously measured by a quadrupole mass spectrometer (Balzers QMS 200, using a calibrated flow-through-capillary).

Gas purities were as follows: O_2 (4.5), CO (4.7), and Ar (5.0). Care was taken of decomposing $Ni(CO)_4$ (present as trace amounts in CO gas cylinders) before usage. X-ray photoelectron spectroscopy (XPS) after activity measurements never indicted the presence of Ni in the sample.

To provide information about (temperature-dependent) initial reaction rates, a second all-glass circulating reactor was used. In this reactor, gases were circulated, over the sample at low pressures and temperatures in order to guarantee low CO conversion. Details of this set-up were provided elsewhere [15]. To condition catalysts, the oxalate precursors were pre-treated in situ in a flow of 10% O_2 in He (50 mL/min) following a similar TPO procedure as described above (heating rate 3 K/min up to 798 K, followed by 20 min of calcination at this temperature). After activation, an amount of 30 mg of the catalyst was used for kinetic testing. The CO oxidation experiments were performed at selected temperatures with 1:1 CO/O_2 gas mixtures in He (9 mbar of both, CO and O_2 and 162 mbar He) during 15 min. Gases were analysed by a quadrupole mass spectrometer after flow-through-capillary (Hiden QMS). The initial rate of CO_2 production was related to the weight of the Ag/TiO_2 samples, the activity was expressed per weight unit of catalyst, i.e. $\mu mol\ s^{-1}\ g_{cat}{}^{-1}$. Each conversion curve was linearly interpolated and one temperature selected (313 K) for which all catalysts were active.

The Ag and Ti contents in the catalyst samples were determined (after TPO measurements) from measurements with a double-focusing inductively coupled plasma mass spectrometer (ICP-MS, Thermo Corp.) using a Meinhard concentric nebulizer connected to a Scott-type spray chamber operating at room temperature. ICP-MS confirmed the composition of the catalysts in terms of % (w/w) of Ag and TiO_2. For example, the Ag and TiO_2 contents of the 10% Ag/TiO_2 sample, after CO oxidation, were $10.07 \pm 0.41\%$ (w/w) Ag and $88.2 \pm 3.0\%$ (w/w) TiO_2 meaning that obviously no Ag was lost during either preparation or reaction.

(High Resolution) Transmission Electron Microscopy (TEM, Philips CM20 and HRTEM, Jeol 3010) was

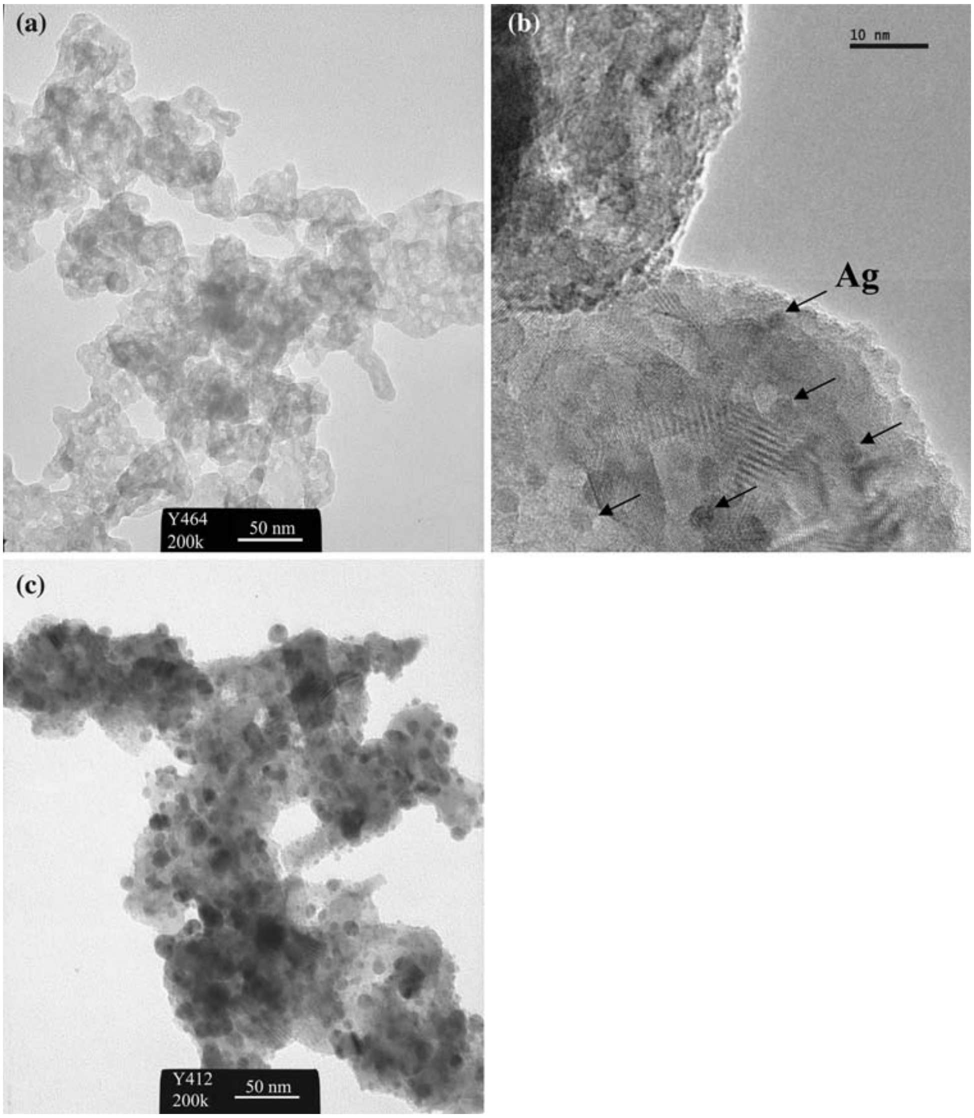

Fig. 1 Transmission Electron Microscopy (TEM) of 2% (**a**), HRTEM of 4% (**b**) and TEM of 10% Ag/TiO_2 catalysts (**c**) after TPO (temperature programmed oxidation) activation and CO oxidation

employed for the structural characterisation of catalysts (at 200 kV acceleration voltage). Samples for TEM were prepared by deposition of a small droplet from an aqueous suspension onto a carbon-coated microgrid. Although a detailed TEM characterization of our Ag/TiO_2 catalysts will be presented elsewhere we mention here that all samples, after TPO and CO oxidation studies, exhibit Ag nano-sized particles except for 2% Ag/TiO_2 where the diffraction-limited image contrast hampers the distinction between Ag-related features and TiO_2 support (Fig. 1a). Catalysts with a higher Ag loading (4 and 10%, respectively) show Ag particles (see arrows in Fig. 1c) in polyhedral morphology with sizes eventually reaching 10 nm in diameter. Figure 1b singles out a region containing a large portion of Ag particles with sizes of 3–4 nm. Quite generally, however, catalyst samples with Ag loadings higher than 2% are characterized by a rather broad distribution of Ag particle sizes. In this context it should be kept in mind that a bright-field TEM analysis of Ag-based catalysts needs much care and can easily lead to erroneous results due to environmental influences before and while imaging, see for example ref. [16].

The activated samples were analysed by X-Ray Diffraction (XRD 500, Bruker) using K_α rays (1,5406 Å) of a copper anode (40 kV, 30 mA). XRD scans were digitally recorded with a stepsize of 0.02° in 1.2 s and evaluated using profile fitting methods. Samples contained TiO_2 nearly exclusively in the anatase form. Very small amounts of rutile and brookite were likewise seen.

The BET surface area of a pure TiO_2 samples were determined either after TPO (including the 20 min heat treatment at 798 K) or TPO and CO oxidation studies. Data were evaluated using the desorption branch of the hysteresis loops. After TPO the surface area of pure TiO_2 was 99 m^2/g using Ar as probing gas. Since it was inactive under the conditions applied in this study no BET measurement after CO oxidation was performed. TPO-activated Ag/TiO$_2$ catalysts generally had lower surface areas. Respective values changed only moderately after CO oxidation measurements. To provide an example, the BET surface area of 10% Ag/TiO$_2$ (the most active catalyst) after TPO was 49 m^2/g while it was 44 m^2/g after CO oxidation at 523 K. Li et al. reported the surface area of mesoporous titanium oxide to decrease rather strongly when adding increasing amounts of Ag [17].

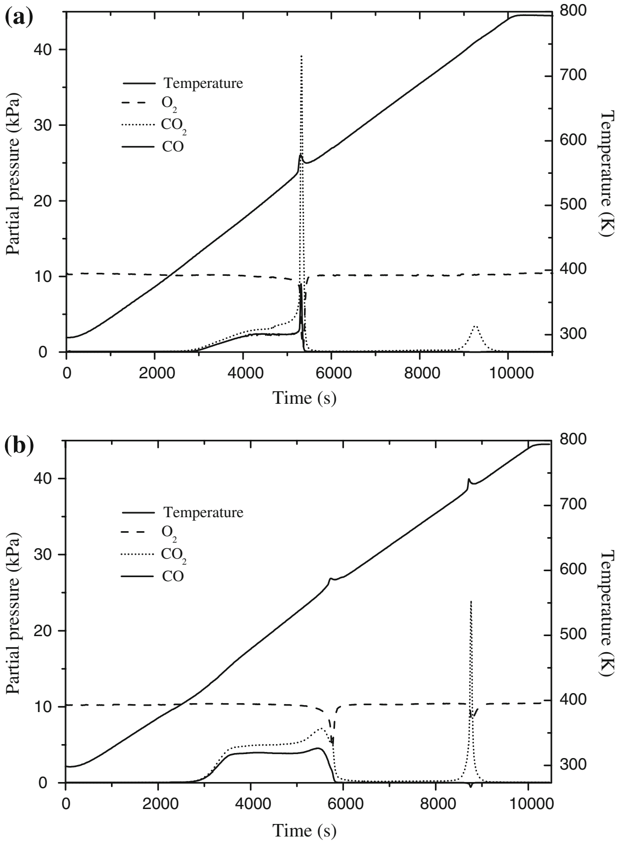

Fig. 2 TPO (temperature programmed oxidation) of co-precipitated Ag-TiO oxalates, (**a**) 2% Ag, (**b**) 10% Ag

3 Results and Discussion

As mentioned above, active Ag/TiO$_2$ catalysts have not been prepared previously via co-precipitation of Ag- and TiO-oxalates. Generally, one of the basic ideas of this method is to achieve intimate mixing of both metals in similar oxalate precursor structures at the instant of precipitation. Subsequent thermal decomposition in the presence of oxygen is then thought to cause oxalate groups to be stripped off as mainly CO$_2$ and to build the oxide structure of the support. This latter process must be regarded as a complicated solid state reaction involving transient TiO$_x$ ($x = 1,\ldots,2$) solid phases with extended defect structures. Such defects are likely present in the final oxide and may probably act as anchoring and nucleation sites for noble metal atoms/particles.

The thermally activated decomposition of the mixed oxalate is of crucial importance and it can be anticipated that the final catalyst structure will depend on the oxidizing conditions applied while heating. In this paper we concentrate on the decomposition of the mixed oxalate by temperature programmed oxidation (TPO) in the presence of 10% O$_2$ in argon. Figure 2a, b provide examples of TPO results for samples with 2 and 10% Ag loading. Quite generally, two distinct features can be identified in both figures, one at high temperature with a peak at around 753 K and another one being broad with an onset at about 423 K and ending in a peak at ~563 K. This latter peak is narrow and no other peak can be observed until the occurrence of the high-temperature peak at 753 K. Both, CO$_2$ and CO are detected at the low-temperature peak while only CO$_2$ appears at high temperature. The peak at 563 K is much more pronounced for the 10% Ag sample (the width at half-height is of ~3 K). For both samples, 2 and 10% Ag, oxygen consumption is observed to coincide with this low temperature desorption peak whereas no such consumption is seen at high temperature. The underlying chemical processes are exothermic as demonstrated by a small temperature rise during decomposition–desorption.

It worth mentioning that, besides CO/CO$_2$ formation, water is observed to be released. The desorption of the latter begins at about 413 K and usually terminates in coincidence with the CO/CO$_2$ peak at 563 K. Obviously, since the oxalate co-precipitation is performed in acetone, the formation of water vapour must be associated with the rupture of structurally bound H$_2$O.

It is also worth mentioning that the TPO spectrum of pure TiO-oxalate, not shown here, contains quite similar CO/CO$_2$ desorption features as those of the co-precipitated Ag/TiO-oxalate. Peaks are observed at ~538 K and ~753 K, the former being much wider than in the Ag/TiO co-precipitated oxalate [18]. Furthermore, a peak at 438 K may be observed the extent of which depends on the actual excess of oxalic acid used for the precipitation. Details on the pure TiO-oxalate thermal decomposition in different atmospheres will be published elsewhere.

TPO experiments with pure Ag$_2$C$_2$O$_4$ in either presence or absence of oxygen have not been performed here (note that this compound has explosive properties [19]). Some of the problems in understanding the (autocatalytic) decomposition of Ag$_2$C$_2$O$_4$ have been described by L'vov [20] but no general agreement seems to have been reached concerning the detailed kinetics of the process.

The TPO spectra shown in Fig. 2 a, b suggest oxalate decomposition to occur stepwise which is in agreement with the Ostwald–Vollmer rule. Accordingly, the formation of

CO during oxalate decomposition leaves oxygen behind, i.e. metal oxides are formed whose composition is not known. The observation that only CO_2 is produced during the high-temperature peak at 753 K suggests oxycarbonate structures to be formed in an intermediate stage of the TPO experiment. The peak is accompanied by oxygen consumption so that we assume that the underlying process is associated with the transformation of oxygen-deficient TiO_{2-x} into TiO_2 (which still contains defects). Note that TPO does not provide any evidence for the formation of Ag_2O. The thermal decomposition of pure $Ag_2C_2O_4$ is usually terminated much below 753 K [21, 22] so that the above assumption of a process involving the $TiO_{2-x} \rightarrow TiO_2$ transformation seems to be a plausible suggestion. On the other hand, we cannot exclude the possibility of compound formation, such as $M(I)_2TiO(C_2O_4)_2 \cdot H_2O$ which is known to exist for $M(I)=NH_4$ [23] and K [24]. To our best knowledge, a compound with M(I)=Ag has not been reported in the literature so far.

We now turn to the kinetic data obtained in studies of the CO oxidation over Ag/TiO_2 catalysts prepared and measured after both TPO and a 20 min treatment in 10% O_2/He at 798 K. Obviously, large differences exist between the CO conversion of 2% Ag/TiO_2 and all other samples. While $T_{50} = 493$ K (temperature of 50% conversion) for the lowest (2% Ag) loading, $T_{50} = 368$ K is achieved for a Ag loading twice as large. The best performance within the series of prepared samples is obtained for 10% Ag/TiO_2 ($T_{50} = 333$ K). The detailed conversion curves are shown in Fig. 3 (except for 4% Ag/TiO_2) and compared to the one of 2% Ag/TiO_2. Obviously, while the 10% Ag sample reaches full conversion at 373 K, a completely different behaviour is seen for the 2% Ag analogue: even at 523 K this latter sample provides a conversion of only 74%. Once the 100% level is reached for samples with higher Ag loading stable performance is obtained up to at least 523 K (or even 573 K as seen by random examination). On the other hand, pure TiO_2 is catalytically inactive until 673 K and therefore not shown in Fig. 3.

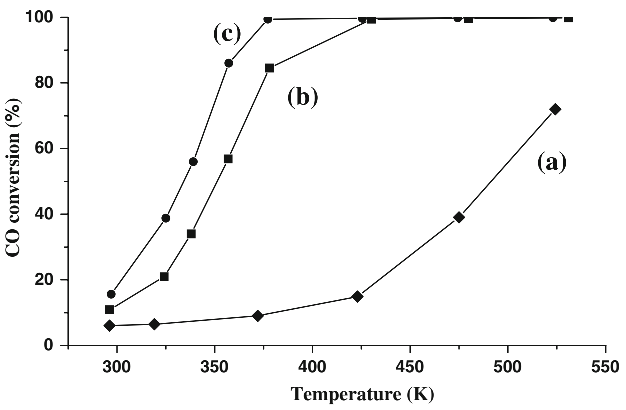

Fig. 3 Conversion vs. temperature for (**a**) 2% Ag/TiO_2, (**b**) 7% Ag/TiO_2 and (**c**) 10% Ag/TiO_2

In order to provide more detailed kinetic insight into the CO oxidation we have performed rate measurements at low conversion using an all-glass circulation reactor. The initial reaction rates for the different catalysts are compiled in Table 1 for a reaction temperature of 313 K for which all catalysts had appropriate activity to allow for a cross-comparison of the samples. The respective time dependence of the reaction rate at 313 K is plotted in Fig. 4 and shows the typical behaviour of progressively decreasing rates as time proceeds (which is due to the consumption of reactants while circulating them). As to be expected from the conversion results presented above, the lowest rate is obtained for the 2% Ag/TiO_2 while the highest is that for the 10% Ag/TiO_2 catalyst. In order to provide (apparent) activation energies the temperature dependence of the initial reaction rates was evaluated at otherwise low conversion (<10%). In this manner linear Arrhenius behaviour was obtained for all samples. Values of the activation energy (E_A) are very similar, i.e. they vary within a range of 13–25 kJ/mol. While such values are not unexpected for highly active catalysts they seem low for catalysts of moderate activity as is, for example, 2% Ag/TiO_2. One tentative explanation could be that while the gross structural features of the catalysts are similar, the number density of active sites for low Ag loading is much smaller.

Table 1 Catalytic activity (μmol s^{-1} g^{-1}) at 313 K for Ag/TiO_2 catalysts with different Ag loading

Sample	r_o (μmol/s*g_{cat}), 313 K
2% Ag/TiO_2	0.37
4% Ag/TiO_2	0.48
7% Ag/TiO_2	1.24
10% Ag/TiO_2	1.48

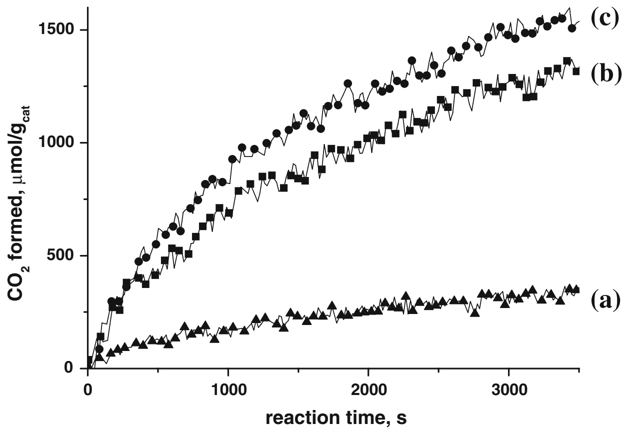

Fig. 4 CO_2 formation in the CO + O_2 reaction on (**a**) 2% Ag/TiO_2, (**b**) 7% Ag/TiO_2 and (**c**) 10% Ag/TiO_2

Following this scenario, the available amounts of Ag(I) first interact with TiO_{2-x} defect sites in 2% Ag/TiO_2 rather than to form a substantial number of nano-sized Ag particles. We also mention that 10% Ag/TiO_2 catalysts seem at present more active than others with significantly larger loading (15% Ag, for example). Respective data will be shown in a future paper along with a characterisation by X-ray photoelectron spectroscopy.

4 Summary and Outlook

A novel method has been developed to prepare active Ag/TiO_2 catalysts via co-precipitation of Ag- and TiO-oxalates. It may be speculated that this co-precipitation initially leads to the formation of $TiO(C_2O_4)_2^{2-}$ derived structures in which Ag(I) takes the role of the counter ion. Thermal decomposition in oxygen may then cause the formation of TiO_{2-x} ($x \rightarrow 1$) with defect-mediated binding of Ag atoms/nanoparticles. The details of the underlying processes are largely unknown and their study beyond the scope of the present Letter. In any case, the bright-field TEM results obtained so far confirm that Ag nanoparticles are present after TPO/CO-oxidation of those samples containing Ag amounts above 2% (w/w). The broad Ag particle size distribution in all these catalysts suggests a particle size effect not to be in operation. This latter point yet needs further clarification, for example by combining high-angular annular dark field imaging with TEM. In this context, note the very different observation according to which small Ag particles seem to be responsible for the NO to N_2 reduction in the presence of hydrogen over Ag/alumina catalysts [25, 26].

Catalysts containing between 4 and 10% (w/w) Ag have demonstrated low-temperature CO oxidation activity whereby $T_{50} = 333$ K has been obtained for the 10% Ag/TiO_2 sample. Different from studies of Ag-based catalysts with supports other than TiO_2, a remarkably stable 100% CO conversion has been observed up to 523 K. In these catalysts the TiO_2 support is predominantly given in the anatase polymorph. The apparent activation energy has been found to be in the range of 13–25 kJ/mol as measured "under static conditions". Detailed spectroscopic characterisation of these catalysts is underway and will help providing an understanding of why Ag/TiO_2 performs that well. We mention at this point in time that TiO_2 can be easily replaced by other supports using an analogous procedure of oxalate co-precipitation. A comparison with Au-based catalysts (which cannot be prepared via the oxalate route) is tempting and will be likewise presented in a forthcoming paper.

Acknowledgments V. Iablokov gratefully acknowledges PhD financial support by "ARC" (Communauté Française de la Belgique). G. Melaet is thankful for a PhD research grant by "FRIA" of the FNRS (Fonds National de Recherche Scientifique, Communauté Française de Belgique). K. Frey has been awarded a grant for short-term post-doctoral research at the ULB which is likewise acknowledged. Part of the work has been performed in the frame of a common COST D36/003/06 project. We also acknowledge the technical help of O. Geszti, Zs. Varga and M.P. Delplancke for providing TEM, ICP-MS and XRD characterisation. We are also grateful to the Hungarian Science and Research Fund OTKA grant Nos. K-68052 and T-049564.

References

1. Haruta M, Yamada N, Kobayashi T, Iijima S (1989) J Catal 115:301
2. Boccuzzi F, Chiorino A (2000) J Phys Chem B 104:5414
3. Haruta M, Tubota S, Kogeyama H, Genet M, Delmon B (1993) J Catal 144:175
4. Valden M, Lai X, Goodman DW (1998) Science 281:1647
5. Lopez N, Janssens TVW, Clausen BS, Xu Y, Mavrikakis M, Bligaard T, Nørskov JK (2004) J Catal 223:232
6. Liu LM, McAllister B, Ye HQ, Hu P (2006) J Am Chem Soc 128:4017
7. Bond GC, Louis C, Thompson DT (2006) In: Hutchings GJ (ed) Catalysis by gold, Chapter 6. Catalysis science series, vol 6, p 161
8. Sarkany A (2005) Colloids Surf A Physicochem Eng Asp 269:67
9. Lippits MJ, Gluhoi AC, Nieuwenhuys BE (2007) Top Catal 44(1–2):159
10. Qu Z, Huang W, Cheng M, Bao X (2005) J Phys Chem B 109:15842
11. Qu Z, Cheng M, Huang W, Bao X (2005) J Catal 229:446
12. Imamura S, Sawada H, Uemura K, Ishida S (1988) J Catal 109:198
13. Xia GG, Yin YG, Willis WS, Wang JY, Suib SL (1999) J Catal 185(1):91
14. Buess P, Caers RFI, Frennet A, Ghenne E, Hubert C, Kruse N (2002) U.S. patent, 6 362 239 B1
15. Frey K (2006) PhD thesis, Budapest
16. Arve K, Svennerberg K, Klingstedt F, Eränen K, Wallenberg LR, Bovin J-O, Capek L, Murzin DY (2006) J Phys Chem B 110:420
17. Li XS, Fryxell GE, Wang C, Engelhard MH (2007) Microporous Mesoporous Mater (in press)
18. Bongiovanni A (2007) PhD thesis, ULB (in preparation)
19. Jander G, Blasius E (1995) lehrbuch der analytischen und präparativen Chemie. Hirzel Verlag
20. L'vov B (2000) Thermochim Acta 364:99
21. Gusev EA, Dalidovich SV, Shandakov V, Vecher AA (1985) Thermochim Acta 89:391
22. Dollimore D, Evans TA (1991) Thermochim Acta 179:49
23. Van de Velde GMH, Harkema S, Gellings PJ (1974) Inorg Chim Acta 11:243
24. Fester A, Bensch W, Trömel M (1994) Acta Crystallogr C 50:850
25. Satokawa S, Shibata J, Shimizu K, Satsuma A, Hattori T (2003) Appl Catal B 42:179
26. Sazama P, Čapec L, Drobná H, Sobalík Z, Dědeček J, Arve K, Wichterlová B (2005) J Catal 232:302